

Supplementary Information

NIR-triggered upconversion and sensitized NIR-emission in Yb-based Eosin Y lakes doped latex nanoparticles

Rita B. Cevallos-Toledo ^a, Delia Bellezza ^a, María González-Béjar ^{a*} and Julia Pérez-Prieto ^{a*}

Instituto de Ciencia Molecular (ICMol), Universitat de València, Catedrático José Beltrán 2, Paterna, 46980 Valencia, Spain.

*Corresponding authors

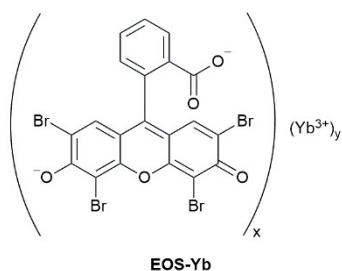
María González-Béjar e-mail: maria.gonzalez@uv.es

Julia Pérez-Prieto e-mail: Julia.perez@uv.es

Materials

Eosin Y (EOS, ~99 %, Sigma Aldrich), Methacrylic acid methyl ester (stabilized with 6-*tert*-Butyl-2,4-xyleneol) (MMA, 99.80%, TCI), Octadecyl acrylate (ODA, 97.00%, Sigma Aldrich), Sodium dodecyl sulfate (SDS, 99.00%, Sigma Aldrich) Potassium persulfate (KPS, 99.00%, Sigma Aldrich), Deuterium oxide (D₂O, 99.90% Eurisotop), Deuterated DMF (DMF-*d*₇, 99.5%, Eurisotop), membrane of regenerated cellulose of 3.5KDa from Spectra/Por®.

EOS-Yb is soluble in DMF and DMSO but it is insoluble in water and was synthesized as previously reported¹.



Scheme S1. Chemical structure of Yb-based Eosin Y lake ([EOS]_x[Yb]_y) (EOS-Yb).

Characterization

Absorption spectra were recorded in a UV/VIS/NIR spectrophotometer Lambda 1050, equipped with PerkinElmer UV Winlab software. The measurements were carried out with precision cells of Quartz SUPRASIL® (light path: 0.1mm).

Steady-state emission spectra and time-resolved kinetics were recorded in a FLS1000 photoluminescence spectrometer (Edinburgh Instruments) equipped with a visible photomultiplier tube (PMT-980, Edinburgh Instruments) and a NIR PMT (H10330C-75, Hamamatsu Photonics K.K.). Four different excitation sources coupled to the system were used for the experiments: the standard 450 W ozone-free xenon arc lamp, a microsecond 60 W Xenon Flashlamp (mF2, Edinburgh Instruments), a vis-NIR pulsed supercontinuum laser (SuperK EXU-6, NKT Photonics), and a continuous wave (CW) laser diode at 980 (2W PSU-III-LED, Changchun New Industries Optoelectronics Technology Co. Ltd. (CNI)). The corrected emission spectra were obtained exciting with Xe lamp

or CW laser diodes and applying the appropriate background, light source, excitation intensity, and detector sensitivity corrections. When recording an emission spectrum, the equipment automatically selects the appropriate longpass filter in the emission monochromator filter wheel to avoid second order artefacts. The filter wheel includes filters for the UV-Vis emission monochromator (410, 680, and 900 nm) and the NIR emission monochromator (410, 680, 1100, and 1200 nm).

Upconversion emission spectra were registered upon excitation with NIR laser diode (980 nm; power density: 8.04 Wcm⁻²), and time-resolved upconversion kinetics were performed by electronically pulsing the 2 W 980 nm laser diode with an extended range pulse width control box (PM-2) at 10 KHz laser frequency and 13.6 μs laser pulse width by means of the multi-channel scaling detection technique (MCS). Laser frequency was selected at the fastest setting possible and the laser pulse width was kept as short as possible but still letting it detect an acceptable signal level (5000–10000 cps). The emission was monitored at 600 nm (9 nm bandwidth) from 0 to 80 μs (1 cycle and 1000 channels). Laser power densities reported for emission spectra were obtained by measuring laser power in the FLS1000 sample chamber with a thermal sensor (S470C, Thorlabs) coupled to a PM100D console (Thorlabs) and the laser spot profile was measured with a LT665 (Ophir) silicon CCD camera (D4σX and D4σY definitions which afforded an approx. 0.19 cm² laser spot area). Spectra were recorded with the following specifications: spectral range of 500–750 nm; step size of 1 nm; accumulation time of 0.1 s, and emission bandwidth of 12 nm.

A tilted *front face* holder was used for all room temperature measurements. Fluoracle software was used to register the data. Mathematical analyses were performed by using Kaleida Graph software. Laser power was measured with a laser power meter PD300-3W and the laser spot size was provided by the manufacturer. Laser power and spot size were divided to provide excitation power density values.

The ICP analysis was performed at the central research support service (SCSIE) of the University of Valencia using an Agilent 7900 ICP-MS unit.

DLS measurements were carried out with Zetasizer Ultra (ZSU5700) from Malvern Panalytical. Data points correspond to mean values from three independent measurements.

Scanning electronic microscopy (SEM) was performed at the central research support service (SCSIE) of the University of Valencia using a Hitachi S4800 microscope operating at 10 kV acceleration voltage.

Absolute quantum yields were measured in a Quantaurus QY Plus (C13534-11, Hamamatsu Photonics K.K.) coupled with a NIR photoluminescence measurement unit (C13684-01, Hamamatsu Photonics K.K.), equipped with a Xenon lamp and an MDL-III-980 laser power of 2.5 W (CNI Opt. Tech. Co. Ltd.), maximum irradiance of 560 ± 30 W cm⁻². The samples were placed in a 1 cm path quartz cell with seal tube. All measurements were performed using DMSO as blank.

XPS spectra were acquired with a VG-Microtech Mutilab 3000 equipment, which has a semispherical electron analyzer with 9 channels, pass energy of (2–200 eV) and an X-ray radiation source with Mg and Al anodes.

Synthesis of EOS NPs

Briefly, 40 mg of EOS were dissolved in 600 μL of deuterated N,N-dimethylformamide (DMF-d7). Then, sodium dodecylsulfate (SDS; 0.3 mmol) dissolved in D₂O was added. The mixture was vigorously stirred for 30 min. Next, octadecyl acrylate (ODA; 0.6 mmol) was mixed with methyl methacrylate (MMA; 46.9 mmol). The monomers were added to the previous mixture, and then vigorously stirred for 30 min to homogenize the mixture. This microemulsion was transferred to a two neck round bottom flask equipped with a condenser, degassed with Ar and heated to 70 °C under stirring for 15 min. Subsequently, potassium persulfate (KPS; 0.4 mmol), previously dissolved in 2.5 mL of D₂O, was added to initiate the free radical polymerization under Ar. Polymerization continued for 45 min under Ar. Then, the mixture was purified by dialysis against milliQ water during 48h with a membrane of regenerated cellulose of 3.5KDa.

Table S1. Nanoparticle size, PDI and optical features of polymeric nanoparticles doped with lanthanide complexes.

Polymer	Synthetic method	Ln	Size (nm)	PDI	λ_{ex} (nm)	λ_{em} (nm)	Stokes Shift (nm)	Anti-Stokes Shift (nm)
PEG/PS ²	Free-radical co-polymerization	Eu	211	1.14	340	614	254	-
		Tb	287	1.07	340	612	272	-
PS ³	Self-assembly	Tb	201	1.04	310	545	235	-
		Eu	152	1.05	310	610	300	-
		Sm	162	1.03	310	646	336	-
PS/AAc ⁴	Emulsion copolymerization	Eu	41	-	340	616	276	-
		Tb	51	-	320	544	224	-
		Sm	46	-	341	645	304	-
		Dy	46	-	318	485	167	-
PS ⁵	Miniemulsion polymerization	Eu	71	0.09	343	613	270	-
PSS ⁶	Polyelectrolyte molecules adsorption	Eu	50-100	-	391	614	224	-
		Yb	50-100	-	391	978	587	-
PMMA-COOH ⁷	Nanoprecipitation	Eu	10-30	-	530	614	84	-
PMMA-co-MAA ⁸	Coprecipitation-assembly	Eu	52	-	412	614	202	-
poly(9-vinylcarbazole) ⁹	Nanoprecipitation	Eu	15-18	-	342	612	270	-
Polystyrene maleic acid ¹⁰	modified microfluidic mixing	Eu	15	-	410	618	208	-
					800	615	-	185
PMMA ¹¹	Microemulsion polymerization	Eu	95-445	0.013-0.06	300	617	317	-
PMMA*	Microemulsion polymerization	Yb	118	0.1	530	573	43	-
					980	574	-	406
					530	978	448	-

*This study.

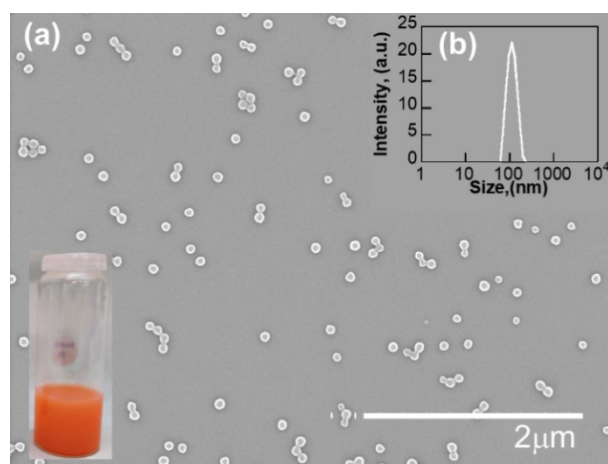


Fig. S1. (a) SEM image and (b) DLS average histogram of EOS NPs. (Hydrodynamic diameter = $107 \text{ nm} \pm 0.8 \text{ nm}$, PDI= 0.05). Inset: Photograph of EOS NPs under laboratory light.

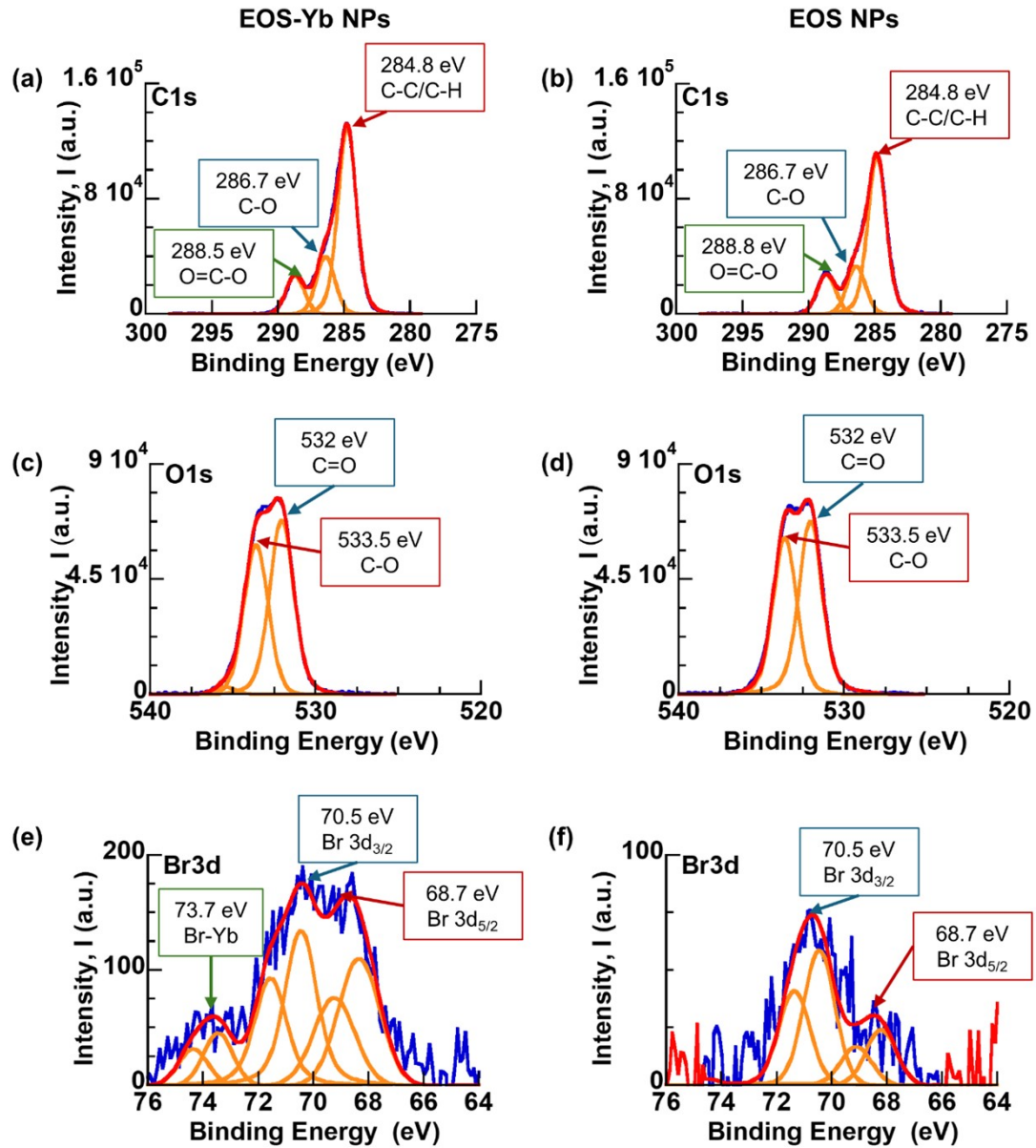


Fig. S2. XPS spectra of C 1s of (a) EOS-Yb NPs (b) EOS NPs and O 1s of (c) EOS-Yb NPs and (d) EOS NPs, and Br 3d of (e) EOS-Yb NPs and (f) EOS NPs Yb 4d.

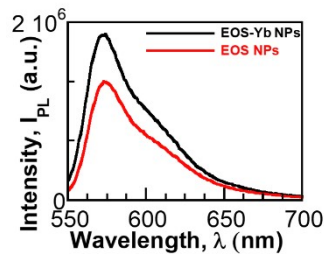


Fig. S3. Comparison of the downshifting emission in the EOS-Yb NPs vs EOS NPs (λ_{ex} =530 nm).

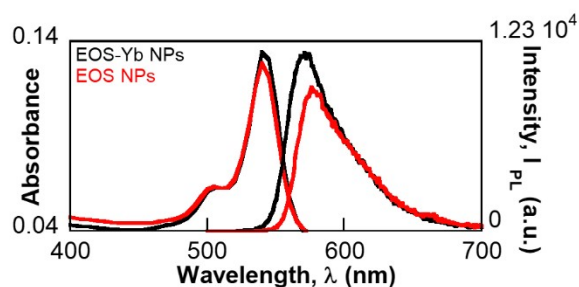


Fig. S4. Comparison of the absorption spectra and upconversion emissions of EOS NPs and EOS-Yb NPs in DMSO- d_6 ($\lambda_{ex}=980$ nm).

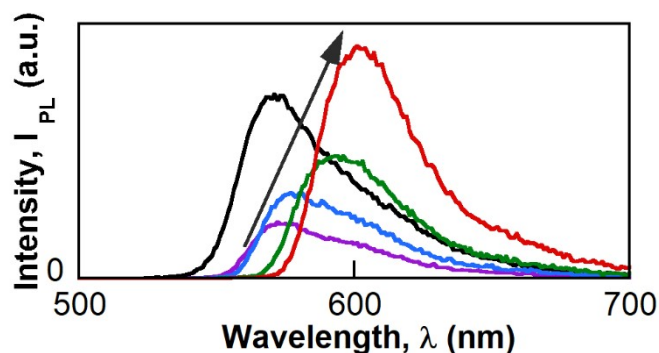


Fig. S5. Comparison of the UC emission ($\lambda_{ex}=980$ nm) of EOS-Yb NPs (black line) and EOS-Yb (1 mg/mL (purple line), 2.5 mg/mL (blue line), 5 mg/mL (green line) and 10 mg/mL (red line)).

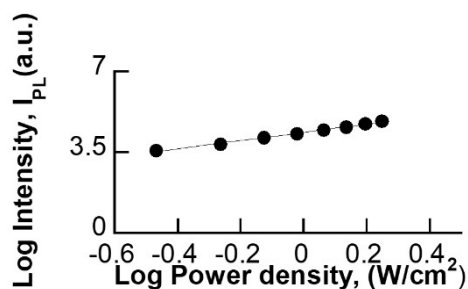


Fig. S6. Linear fit of log emission area vs log laser power density of EOS-Yb NPs in DMSO- d_6 ($\lambda_{ex}=980$ nm)

References

- 1 R. B. Cevallos-Toledo, D. Bellezza, J. Ferrera-González, A. Giussani, E. Ortí, M. González-Béjar and J. Pérez-Prieto, *ChemPhotoChem*, 2023, **7**, 1–7.
- 2 K. Tamaki and M. Shimomura, *Int. J. Nanosci.*, 2002, **01**, 533–537.
- 3 K. Tamaki, H. Yabu, T. Isoshima, M. Hara and M. Shimomura, *Colloids Surfaces A Physicochem. Eng. Asp.*, 2006, **284–285**, 355–358.
- 4 P. Huhtinen, M. Kivela, O. Kuronen, V. Hagren, H. Takalo, H. Tenhu and H. Ha, 2005, **77**, 2643–2648.
- 5 J. Desbiens, B. Bergeron, M. Patry and A. M. Ritcey, *J. Colloid Interface Sci.*, 2012, **376**, 12–19.
- 6 R. R. Zairov, A. P. Dovzhenko, A. S. Sapunova, A. D. Voloshina, D. A. Tatarinov, I. R. Nizameev, A. T. Gubaidullin, K. A. Petrov, F. Enrichi, A. Vomiero and A. R. Mustafina, *Mater. Sci. Eng. C*, 2019, **105**, 1–10.
- 7 M. Cardoso Dos Santos, A. Runser, H. Bartenlian, A. M. Nonat, L. J. Charbonnière, A. S. Klymchenko, N. Hildebrandt and A. Reisch, *Chem. Mater.*, 2019, **31**, 4034–4041.
- 8 G. Shao, R. Han, Y. Ma, M. Tang, F. Xue, Y. Sha and Y. Wang, *Chem. - A Eur. J.*, 2010, **16**, 8647–8651.
- 9 W. Sun, J. Yu, R. Deng, Y. Rong, B. Fujimoto, C. Wu, H. Zhang and D. T. Chiu, *Angew. Chemie - Int. Ed.*, 2013, **52**, 11294–11297.
- 10 W. Yang, L. M. Fu, X. Wen, Y. Liu, Y. Tian, Y. C. Liu, R. C. Han, Z. Y. Gao, T. E. Wang, Y. L. Sha, Y. Q. Jiang, Y.

- Wang and J. P. Zhang, *Biomaterials*, 2016, **100**, 152–161.
- 11 N. Wartenberg, O. Raccurt, D. Imbert, M. Mazzanti and E. Bourgeat-Lami, *J. Mater. Chem. C*, 2013, **1**, 2061–2068.